DOI: 10.1002/ ((please add manuscript number))

Full Paper

Membrane-Free Detection of Metal Cations with an Organic Electrochemical Transistor

*Shofarul Wustoni[1], Craig Combe[2], David Ohayon[1], Mahmood Hassan Akhtar[1], Iain McCulloch[2,3], and Sahika Inal**

Dr. S. Wustoni, D. Ohayon, Dr. M. H. Akhtar, Prof. S. Inal
King Abdullah University of Science and Technology (KAUST), Biological and Environmental Science and Engineering, Thuwal 23955-6900, Saudi Arabia.

Dr. C. Combe, Prof. I. McCulloch
King Abdullah University of Science and Technology (KAUST), Physical Science and Engineering, KAUST Solar Center, Thuwal 23955-6900, Saudi Arabia.

Prof. I. McCulloch
Department of Chemistry and Center for Plastic Electronic, Imperial College London, London, SW7 2AZ, United Kingdom.

E-mail: sahika.inal@kaust.edu.sa

Keywords: organic electrochemical transistors; bioelectronics; ion sensor; conjugated polymer; crown ether.

Abstract

Alkali-metal ions are the messengers of all living cells, governing a cascade of physiological processes through the action of ion channels. Sodium (Na^+) and potassium (K^+) are the two alkali metals found in human blood serum. Devices that can monitor, in real time, the concentrations of these cations in aqueous media are in demand not only for the study of cellular machinery and dysfunctions, but also to detect conditions in the human body that lead to electrolyte imbalance, such as hypernatremia, hyperkalemia or dehydration. In this work, we developed conducting polymers that respond rapidly and selectively to varying concentrations of Na^+ and K^+ in aqueous media. These polymer films, bearing crown-ether-functionalized thiophene units specific to either Na^+ or K^+ ions, generated an electrical output proportional to the cation type and concentration. Using electropolymerization, we deposited the ion-selective polymers onto microscale gold patterns and integrated them as the gate electrode of an organic electrochemical transistor (OECT). The OECT current changed with respect to the concentration of the ion to which the polymer electrode was selective. Designed as a single, miniaturized chip, the OECT enabled the selective detection of Na^+ and K^+ within a physiologically relevant range. These electrochemical ion sensors required neither a complex functionalization route to fabricate, nor ion-selective membranes or a reference electrode to operate. Such customized conducting polymers have the potential to surpass existing technologies for the detection of alkali-metal ions in aqueous media and for further development into implantable medical devices.

1. Introduction

The cations sodium (Na^+) and potassium (K^+) are the primary ions that cells in mammalian organisms use to communicate with one another. They play a crucial role in numerous biological and physiological processes, such as metabolic transport and the function of nerves and muscles. [1,2] Abnormal levels of these cations in bodily fluids such as sweat, urine, or blood can indicate a variety of dysfunctions, including kidney or heart failures, uncontrolled diabetes, or dehydration.[3] Therefore, *in vitro* monitoring of the electrolyte balance is already a routine part of clinical evaluations. *In vivo* sensing of these cations, using optical sensors or kits reporting fluorescence and colorimetric readouts, can also provide a wealth of information as biological phenomena are studied *in situ*.[4-7] Sensors with sub-second responses permit to follow extracellular ion concentrations and, hence, activities of ion channels, informing about the onset of pathological conditions. However, these ion sensing methods require expensive optical labels, bulky equipment, and experienced personnel to acquire data, and they also typically operate within a range of short excitation wavelengths that is incompatible with biological tissues. [8]

Electrical methods of monitoring cations have a proven track record of being portable, nondestructive, and label-free. Unfortunately, today's commercially available electronic ion sensors rely on decades-old technology, which limits their applications to *in vitro* platforms. These sensors are comprised of an electrode coated with an ion-selective polymeric membrane (ISM). The ISM creates a measurable interface potential at the electrode by selectively taking up ions from an electrolyte.[9,10] To build miniaturized ion sensors, ISMs have been integrated into field effect transistors (FETs) which inherently amplify signals.[11] While ion selective FETs show high performance, patterning ISMs on miniaturized surfaces is not a particularly high-yield process. In addition, pre-conditioning of the devices in a specific electrolyte is usually necessary to minimize potential drifts.[12] In some cases, potential drifts are caused by weak adhesion of the membrane to the transducer surface, interfering with the actual read-out

of the sensor.[13] Another issue arises from the membrane-coating procedure itself, which involves organic solvents and chemical treatments that may be incompatible with the electrode and channel materials underneath, limiting the materials that can be used as transducing units.[14] Hence, the development of a functional, single-component electronic material that can selectively capture ions in an aqueous environment, and then generate an electrical output proportional to the amount of these ions, is a leap forward towards robust electrical sensing of hydrated ions.

Conjugated polymers (CPs) are promising electronic materials for ion sensing. Firstly, the films can be designed to exhibit semi-permeability to hydrated ions.[15-17] Secondly, the doping state of a CP film (and, hence, its conductivity) is typically sensitive to either the polarity or the valence of the ions. Without appropriate functionalization, however, CPs lack the specificity necessary to build an ion sensor. Ever since Pedersen's Nobel Prize-winning work in 1967, [18] functionalization with crown ether molecules, whose selectivity depend on their size, has been a means to render CPs ion selective.[19-23] The first ion-selective CP film was demonstrated by Dabke *et al.* who physically adsorbed a crown ether with a particular affinity for K^+ onto a CP film.[24] The intercalation of the crown cavity by the K^+ ions led to a high local electrostatic field, perturbing the π-conjugation system and resulting in a material that could electrochemically switch in the presence of low concentrations of K^+ (10^{-7} M). However, the operation was irreversible due to the ionophore diffusing out of the film. Therefore, the studies that followed up covalently integrated crown ethers into the CPs.[25] The majority of these materials were used in the solution-state due to the limited interactions of the ions with the films and the detection was based on optical signals. Only a few ionophore-functionalized CPs have made it into solid-state devices that produce an electrical signal proportional to the concentration of a specific ion, yet they mostly operate in organic solvents rather than in aqueous.[26-28] These ion-selective CP films require long incubation times to generate a detectable response, precluding their practical use.[29]

The organic electrochemical transistor (OECT) is an electrolyte gated transistor that leverages the coupling between ionic and electronic charges in CPs and is particularly suited for sensing hydrated ions. In an OECT, a CP film is used in the transistor channel, while a metal is used as the gate electrode. The electrolyte has a direct interface with the channel and the gate electrode. The CP film, which is permeable to the electrolyte ions, translates small changes in ionic fluxes (controlled by the gate electrode) into large changes in its conductivity.[30] To render the OECT ion-selective, ISMs[31-33] and lipid membranes with ion channels[34] can be coated on top of the CP-film channel. For instance, in one study, a polyvinylchloride-based K^+-selective membrane was deposited on top of an OECT channel, transporting only K^+ ions.[33] In this OECT, the applied gate voltage led to changes in the drain current that bore a quantitative relationship to the K^+ concentration of the electrolyte.[33] Despite the competency of OECTs for ion sensing, interposing an ISM vertically in between the microscale channel and gate electrode has been impractical, as in the case of FETs, and their operation is not robust. These technical challenges prevent both widespread use of this technology and its adaptation for applications beyond *in vitro* diagnostics.

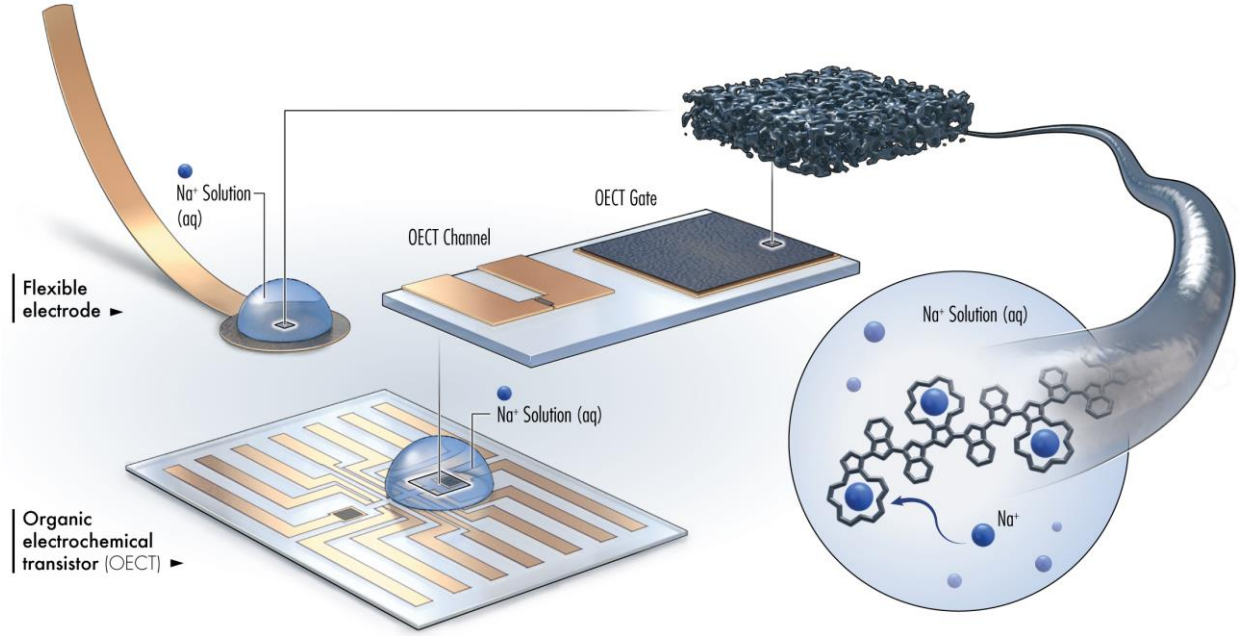

Figure 1. The ion-selective CP film is applied as (i) a flexible, amperometric electrode and (ii) the gate electrode of a microfabricated organic electrochemical transistor (OECT). In the OECT, the CP-based gate electrode renders the device selective towards either Na^+ or K^+ ions. One of the gate electrodes on the OECT chip contains the Na^+-selective CP, whereas the other contains K^+-selective CP. The schematic illustrates the Na^+-selective CP as an example.

In this work, we developed single-component CPs that are involved in both the recognition of a particular cation and the signal-transduction process. Using such CPs, we sought to gain dramatic improvements in the ion sensing performance of OECTs. Our CPs were functionalized with crown ether units that molecularly interacted with either Na^+ or K^+ ions. Using electropolymerization, we patterned these CPs onto platforms with different geometries (Figure 1): i) flexible, macroscale electrodes and ii) rigid, miniaturized gate electrodes of an OECT. As an amperometric, macroscale electrode, the current of the CP film was proportional to the concentration of the ion of interest (Na^+ or K^+) in the measurement solution and showed a negligible response to other cations. When the CPs were integrated as the lateral, miniaturized

gate electrode of an OECT, the device displayed remarkable selectivity and sensitivity towards Na^+ or K^+, across a broad dynamic range, and outperformed other transistor technologies incorporating ISMs. Using a miniaturized OECT chip, as illustrated in Figure 1, we could measure variations in the concentration of these two cations in a blood serum sample in real-time. These devices require neither a complex functionalization route to fabricate, nor ion-selective membranes or a reference electrode to operate. This is the first demonstration of functionalized CPs in OECTs for dual cation sensing. Such ion-selective CPs offer a direct route towards large-scale production and adaptation into different geometries for both *in vivo* and *in vitro* detection of alkali-metal ions.

2. Results and Discussion

2.1. Optimization and Characterization of Ion-Selective CPs

The Na^+-selective monomer, 3,4-(15-crown-5)thiophene (T15c5), and the K^+-selective monomer, 3,4-(18-crown-6)thiophene (T18c6), were synthesized following a procedure previously reported in the literature[36] until the last step, when a modified copper-catalyzed decarboxylation was used (Figure S1).[37] Scheme 1 shows the chemical structures of random copolymers of T15c5 and T18c6 with EDOT, named as p(T15c5-*ran*-EDOT) and p(T18c6-*ran*-EDOT), respectively. Electropolymerization led to the direct incorporation of the ionophore within the conducting polymer network. Steric hindrance of the bulky crown ether units and conformational disorder of the π-electron conjugation necessitated the use of a co-monomer for the electropolymerization of the ion-selective CPs.[38] We chose EDOT as the co-monomer because of its electron-rich nature (i.e., facile electropolymerization with different anions in various media), an ionization potential similar to that of the crown-ether-modified analogue, and the high conductivity and electrochemical stability of PEDOT films. The two monomers have the same reactivity at the coupling sites, which is expected to result in a random

copolymer. We also expected the presence of EDOT in the backbone to lead to a less dense crown ether composition. Such an architecture was reported to reduce the steric effects upon complexation with cations, which might otherwise hinder the counter ion drift towards the backbone.[39] To form a homogenous film, the EDOT weight in the monomer mixture had to be at least twice that of the T15c5 and T18c6.

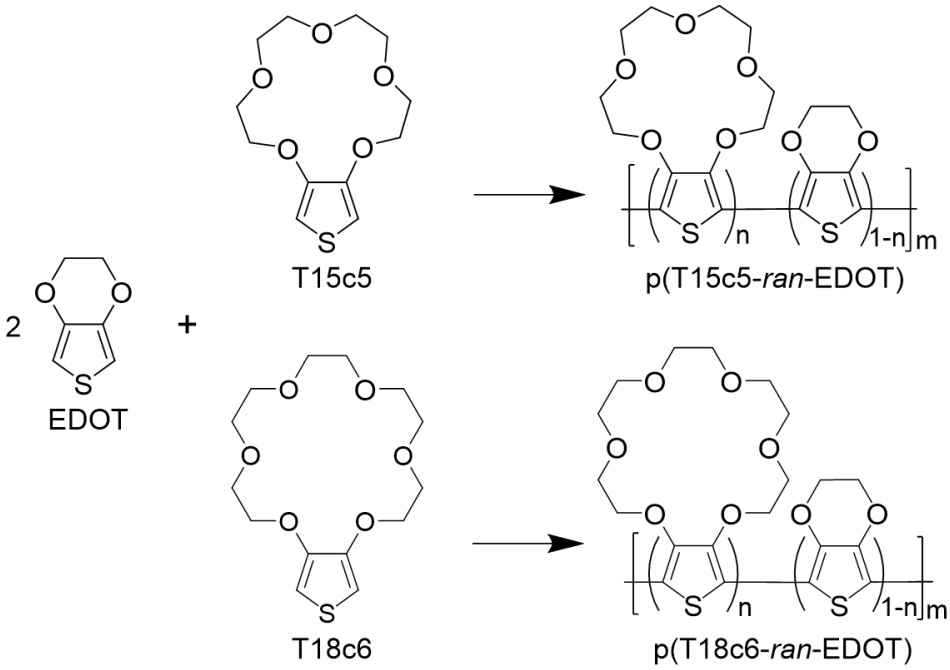

Scheme 1. Chemical structure of the Na^+-selective p(T15c5-*ran*-EDOT) and K^+-selective p(T18c6-*ran*-EDOT). The copolymers were electropolymerized from a mixture of 3,4-ethylenedioxythiophene (EDOT) with either T15c5 or T18c6 on top of Au coated electrodes. The weight of EDOT was double of the crown-ether monomers. Tetrabuthylammonium perchlorate (TBAP) was used as the anionic dopant.

The method of electropolymerization strongly influences the physical and electrical properties of deposited films.[40] Therefore, we screened three commonly applied electropolymerization modes (potentiodynamic, potentiostatic and galvanostatic). We, then, inferred the cation sensitivity of these films from the amplitude of the reduction peak in their cyclic voltammetry (CV) curves recorded in the target electrolyte. In the potentiodynamic mode, we polymerized

the material by applying voltage sweeps within a predetermined potential range (Figure S2a-c). The increase in the current with consecutive CV cycles evidenced the formation of the conducting film on the Au surface. We also used the galvanostatic mode for electropolymerization at a constant current density, as well as the potentiostatic mode which applies a fixed voltage (Figure S2d and e). Figure 2a shows a typical CV curve from a Na^+-selective CP film deposited on an Au-coated flexible substrate recorded in aqueous NaCl solution (10 mM). The reduction peak at ca. 0.4 V arises because the polymer is de-doped by Na^+ ions during the reverse scan. The electrochemical reduction of the p(T15c5-*ran*-EDOT) film from its oxidized state to the neutral state is described by the following reaction:

$$\text{p(T15c5-}ran\text{-EDOT)}^+\text{:}ClO_4^- + Na^+ + e^- \leftrightarrow \text{ p(T15c5-}ran\text{-EDOT)}^0 + Na^+\text{:}ClO_4^- \quad (1)$$

where e^- denotes the electrons injected from the Au electrode underneath the film. According to this relation, the reduction current scales with the number of Na^+ ions penetrating the polymer bulk. Thus, the polymer with the highest reduction current should be the one that incorporates the highest number of Na^+ ions, i.e., that is the most sensitive CP. Figure 2b compares the charge density of the CP films fabricated via these three electropolymerization modes when they are subject to a de-doping bias at 0.4 V. The potentiostatic mode yielded the most sensitive electrodes, i.e., the highest reduction current. Among the scanned voltage ranges, we found that electropolymerization at 1.2 V resulted in the most sensitive films (Figure S2a-c). We observed similar results for the K^+-selective CP. These findings are in line with other reports demonstrating that electropolymerization at a voltage close to the oxidation potential of EDOT (ca. 1.2 V) produces PEDOT-based films with high electrochemical performance.[41, 42]

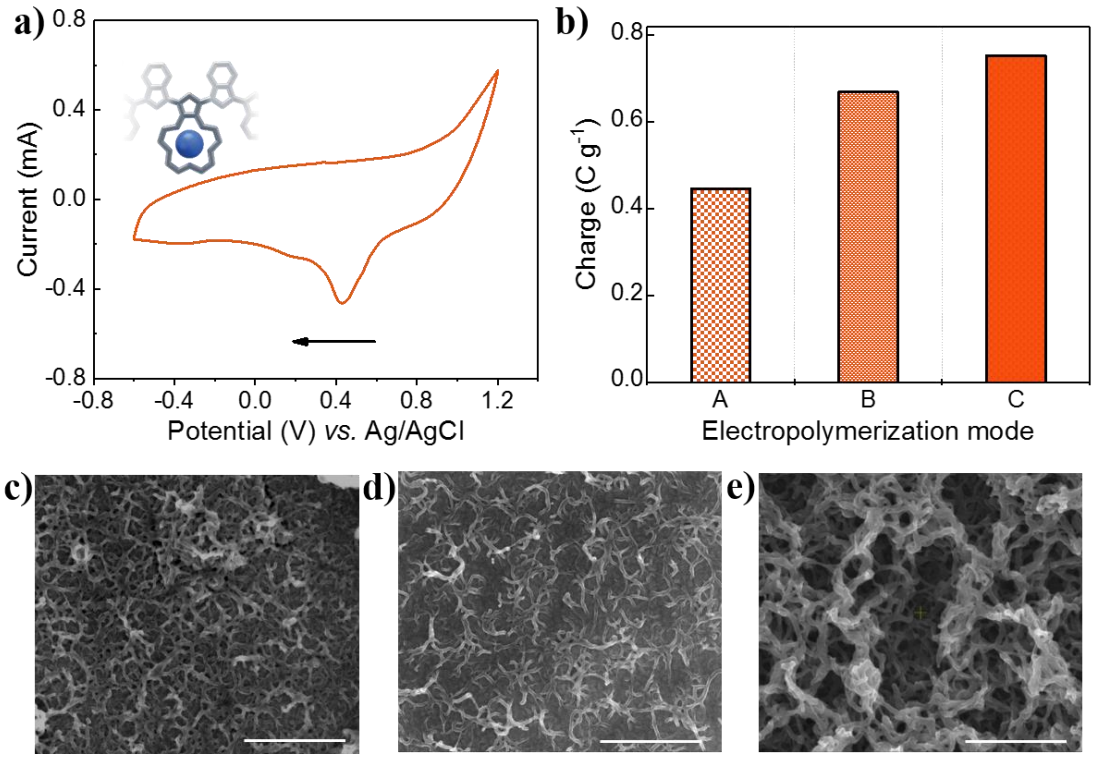

Figure 2. Electrochemical characteristics and SEM characterization of the p(T15c5-*ran*-EDOT) films deposited on Au. **a)** A typical CV curve of the p(T15c5-*ran*-EDOT) electrode displaying a sharp reduction peak in aqueous NaCl solution (10 mM). Inset schematic shows the intercalation of a Na^+ ion with the crown ether. The arrow indicates the direction of the voltage scan. **b)** The charge generated by p(T15c5-*ran*-EDOT) films at 0.4 V *vs*. Ag/AgCl in NaCl solution. A, B, and C are films electropolymerized using the potentiodynamic, galvanostatic, and potentiostatic modes, respectively, and have the same geometry. SEM images of p(T15c5-*ran*-EDOT) films prepared via the **c)** potentiodynamic, **d)** galvanostatic, and **e)** potentiostatic modes. Scale bar is 1 µm.

Like the electrochemical performance, the architecture of the films changed depending on the electropolymerization mode. The films that were deposited via the potentiodynamic (Figure 2c) and galvanostatic modes (Figure 2d) exhibited a branch-like morphology with stacked layers. The potentiostatic mode, on the other hand, resulted in a polymer film that had a three-dimensional microporous structure with interconnected, fibrous features (Figure 2e). A similar

morphology is observed for p(T18c6-*ran*-EDOT) film as well as for pristine PEDOT (Figure S3a and b, respectively). The porous surface morphology is expected to provide a large surface area, allowing the cations to easily penetrate the polymer. These cations then migrate throughout the water-swollen porous structure, in the presence of crown ethers, they get captured by these units, effectively de-doping the polymer. Another parameter that can affect the ion sensitivity of the films is the comonomer feed ratio. We thus electropolymerized p(T15c5-*ran*-EDOT) films via the potentiostatic mode from a variety of comonomer feed ratios. Although all films exhibited fairly identical porous structures (Figure S3c-e), with an increase in the crown ether content of the monomer mixture, the sensing performance also improved (i.e., higher reduction currents). Therefore, we chose to prepare the films from the highest T15c5 or T18c6:EDOT comonomer feed ratio possible, i.e., 2:1. The FTIR spectra shown in Figure S4 evidence the successful copolymerization of the monomers at this ratio. Since crown ether units has larger ring size and introduce electronegative oxygen atoms into the structure, the force constant of the C-O-C bond become higher in the ion-selective polymers compared to the pristine PEDOT, resulting in a shift in the characteristic peak positions to higher wavenumbers (Table S1).

2.2. Ion-Selective CP electrodes

To evaluate the ion selectivity of the CP polymers deposited on flexible Au electrodes shown in Figure 1, we monitored their electrochemical response to equivalent concentrations of Na^+, K^+, and Li^+. Figure 3a demonstrates the reduction current of the electrodes measured in NaCl, KCl, and LiCl (aqueous, 10 mM) upon application of a short de-doping pulse. For p(T15c5-*ran*-EDOT), Na^+ ions generated a higher current readout than the K^+ and Li^+ ions. For p(T18c6-*ran*-EDOT), we measured the highest current in KCl. The PEDOT homopolymer film (i.e., crown ether-free), on the other hand, did not demonstrate a specific response to any particular cation. To understand the extent of the ionophore-cation interactions, we recorded the Raman

as well as XPS spectra of pristine PEDOT and the Na^+-selective copolymer film before and after their exposure to the target electrolyte. Figure S5 illustrates that the Raman spectrum of a p(T15c5-*ran*-EDOT) film incubated overnight in NaCl solution is significantly different from that of the dry film (see the shift of the band at 1425 cm^{-1}, which we attribute to the symmetrical vibration of C=C of the thiophene chains). In contrast, such spectral changes are subtle for the PEDOT film, though it was treated identically. In addition, only for the p(T15c5-*ran*-EDOT) film left overnight in NaCl solution, we detect a clear peak at 1071 cm^{-1} in high resolution XPS spectrum of Na 1s (Figure S6). This peak is attributed to Na ions.[43] Taken together, these findings suggest that the crown ethers of the CP film have strong interactions with their respective cations, which drag them closer to the conjugated units. Thus, the reduction currents of the ion-selective CPs are maximized in the presence of their target cations, while the penetration of other cations is impaired or insignificant.

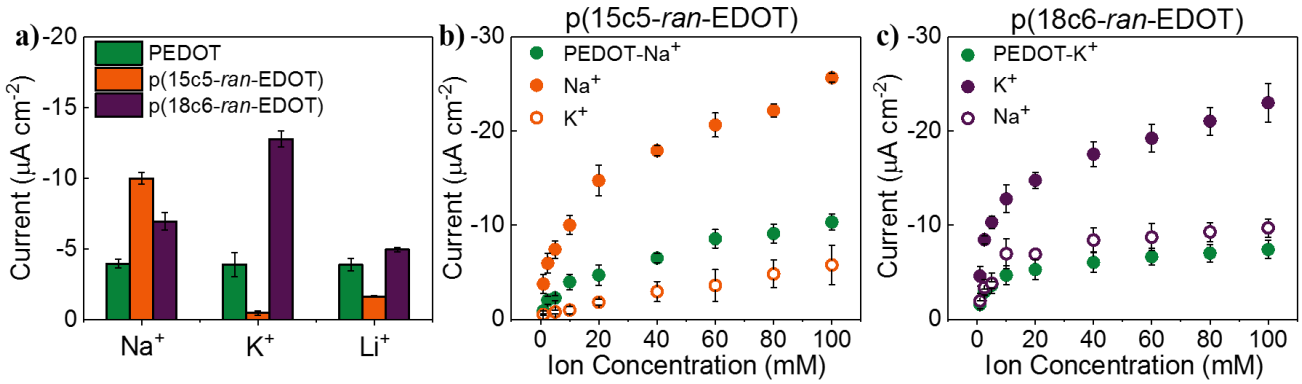

Figure 3. The sensing performance of ion-selective electrodes. **a)** The reduction current of the p(T15c5-*ran*-EDOT) and p(T18c6-*ran*-EDOT) films as well as of the PEDOT homopolymer (i.e., crown ether-free) measured in NaCl, KCl, and LiCl (10 mM, aqueous). The reduction current was recorded upon application of a de-doping potential of -0.3 V *vs*. V_{OC} for 60 s. Real-time response of **b)** p(T15c5-*ran*-EDOT) and **c)** p(T18c6-*ran*-EDOT) electrodes to increasing concentrations of Na^+ or K^+ in the electrolyte. The green symbols represent the dose curve of the PEDOT electrode to the target cation. The error bars were extracted from three devices. The

electrode area (*A*) and film thickness (*d*) are the same for all polymer films, where *A* = 38.48 mm^2 and *d* = ca. 80 nm.

To investigate the selectivity for a large range of concentrations, we recorded the dose curves. Figure 3b shows that the reduction current of p(T15c5-*ran*-EDOT) increased gradually with the concentration of Na^+ ions, with a dynamic range from 1 mM to 100 mM. The curve has two linear regions, with a sensitivity of 570 nA mM^{-1} and 130 nA mM^{-1} for the ranges of 1 – 20 mM and 20 – 100 mM, respectively. For the same concentrations of KCl, the response was significantly smaller, with a sensitivity of 56 nA mM^{-1}. For a broad range of NaCl concentrations (1 – 20 mM), the reduction current of p(T15c5-*ran*-EDOT) was around four times higher than that of the pristine PEDOT. Figure 3c shows the same experiments performed with p(T18c6-*ran*-EDOT). The K^+-selective electrode also produced two linear regions with a sensitivity of 800 nA mM^{-1} and 110 nA mM^{-1} for the ranges of 1 – 10 mM and 10 – 100 mM of K^+, respectively. The electrode was less sensitive to Na^+, especially at high concentrations: 518 nA mM^{-1} (1 – 10 mM) and 36 nA mM^{-1} (10 – 100 mM). Moreover, neither of the electrodes were sensitive to Li^+, the weak current response seen in Figure 2a saturated for concentrations of Li^+ above 10 mM (Figure S7). Both CPs were, however, unresponsive to cations in the micromolar range (< 1 mM). No reduction peak could be resolved in the CV curves, and the current response to the de-doping pulse was close to the value obtained in ultrapure water.

2.3. Ion-Selective OECTs

The flexible electrodes characterized above contained the ion-selective CPs deposited on a macroscale area. Despite their high currents and ease of fabrication and operation, passive electrodes are not particularly suitable for applications that require small penetrating sensors due to the decrease in read-out signals with electrode size. The sensitivity of transistors, on the other hand, is unaffected by miniaturization. To leverage the inherent amplification of the

transistor circuity, we deposited our polymers onto microscale Au patterns of an OECT chip (Figure 1). Then, we used these electrodes to gate OECT channels made of PEDOT:PSS. A schematic of the device fabrication and layout is depicted in Figure S8. In an OECT, in the absence of a gate voltage (V_G), a large current flows in the PEDOT:PSS channel. To turn the device OFF, a positive voltage is applied at the gate electrode which drives cations into the channel. As electrons are injected from the drain, these cations electrostatically compensate the PSS sites. The result is a decrease in the source-drain current (I_D). Figure 4a shows the transfer curve (I_D *vs.* V_G) as well as the transconductance values ($g_m = \Delta I_D / \Delta V_G$) of such a PEDOT:PSS channel gated by p(T15c5-*ran*-EDOT) in 10 mM of KCl or NaCl solution. The output characteristics of this device are shown in Figure S9. When the Na^+-selective polymer gated the channel, we measured higher current and transconductance values in NaCl than in KCl. The differences were more striking as the gate voltage became more negative. This is reasonable considering that at negative voltages, cations drift towards the gate electrode. When the same channel was gated by a PEDOT electrode (i.e., crown ether-free) having the same geometry as p(T15c5-*ran*-EDOT), the device characteristics were independent of the electrolyte type (Figure 4b). Nevertheless, the current of all the tested OECTs varied with the electrolyte concentration (100 nm to 1 M), while selectivity to the cation type was achieved only when we employed the ion-selective CPs as the gate (Figure S10). Similar trends were measured for the channel gated by the K^+-sensitive CP (Figure S11).

Lin et al. studied the ion-sensitive properties of Ag/AgCl-gated OECTs, finding that the transfer curves shift to lower gate voltages with an increase in cation concentration.[17] In agreement with our results for PEDOT-gated OECTs in Figure 4b, they reported that the device response was not selective to the cation type because Ag/AgCl lacks the functionality of interacting only with a particular ion. A few other studies, using conventional electrode materials at the gate, reported the selectivity of the OECT to the cation size and charge, but not the type.[15, 31, 44]

Here, we use a gate electrode containing crown ethers that capture target cations and generating a current specific to the concentration of these cations (Figure 2a). Figure 4c shows that under the same operation conditions, the gate current (I_G) of a PEDOT-gated OECT was significantly lower than that of the device gated by the Na^+-selective CP due to the Faradaic processes of the latter. The I_G of the Na^+-selective OECT decreased stepwise as the Na^+ concentration increased from 10^{-5} M to 1 M. These chelation events then modulated I_D that was orders of magnitude larger than I_G and bore a quantitative relationship with the cation concentration.

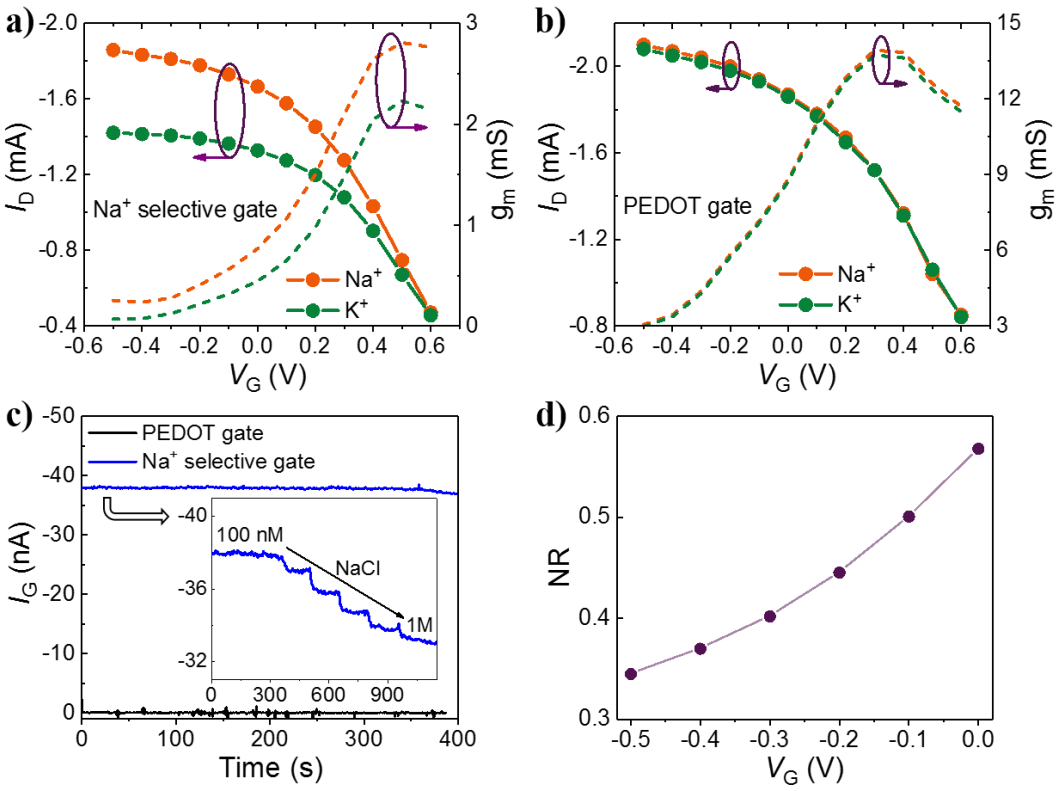

Figure 4. Steady-state characteristics of an OECT with PEDOT:PSS in the channel and p(T15c5-*ran*-EDOT) as the gate electrode. Transfer curves (I_D *vs.* V_G) and transconductance (g_m) characteristics of the channels gated by **a)** the p(T15c5-*ran*-EDOT) electrode and **b)** the pristine (i.e., crown-ether-free) PEDOT electrode in NaCl (orange) or KCl (green) (10 mM). The source-drain voltage (V_D) was -0.1 V. **c)** The change in the gate current (I_G) upon successive additions of Na^+ into the measurement solution when the gate electrode was p(T15c5-*ran*-

EDOT) (blue) or the pristine PEDOT (black). V_D and V_G were -0.1 V. **d)** The normalized response (NR) of the OECT as a function of V_G.

2.4. Real-Time Cation Detection Using the OECT

Figure 4d shows the normalized response (NR) of the Na^+-selective OECT at different gate voltages. These results show that the sensor had the highest sensitivity when biased at a low V_G. A low operating voltage is beneficial for ion sensing: it minimizes energy consumption, ensures operational stability, and eliminates oxidation/reduction of biological species present in complex media.[45, 46] In Figure 5a-b, we show how the OECT current responded, in real-time, to incremental additions of Na^+ and K^+ into the measurement solution. We biased the two ion-selective gate electrodes at -0.1 V and extracted the dose curves for each cation (Figure 5a-b, insets). The OECT response to a change in ion concentration was almost instantaneous, eliminating the need to incubate the device with the measurement solution for extended periods. The sensitivity of the OECT gated with the Na^+-sensitive CP (Na^+ sensor) to Na^+ in the range of 10^{-5} M – 1 M was 0.022 dec^{-1}. The device still responded to K^+ ions, but the linear regime of the calibration curve was now confined to a narrower concentration range of 10^{-3} M – 1 M with a sensitivity of 0.019 dec^{-1} (Figure 5a). Next, we measured the response of the same channels to the same solutions, but this time gated with the K^+-sensitive CP. The sensitivity of the K^+ sensor to K^+ was 0.024 dec^{-1} in the range of 10^{-4} M – 1 M, while its sensitivity to Na^+ was 0.019 dec^{-1} confined to a smaller dynamic range of 10^{-3} M – 1 M (Figure 5b).

Having identified the detection range and sensitivity of the sensors, we evaluated the performance of the OECT when detecting cations in a complex medium: a human-serum sample (Figure 5c). Both the Na^+ and K^+ sensors operated in serum: we measured an increase in the NR as the salt concentration increased within a physiologically relevant concentration range for each cation (Figure 5c). Then, we integrated the two gates by exposing them to the same human-serum sample and performed simultaneous system-level measurements with salt mixtures

added to this sample (Figure 5d). These salt concentrations were chosen to be below and above the threshold values that indicate electrolyte imbalance in the body.[47] While both sensors could detect small changes in target cation concentrations in the human serum sample ("total response"), they were somewhat sensitive to the interfering cation which could cause an overestimation of the actual cation concentrations. This was particularly a concern for estimations of K^+, as its concentration in blood is about one order of magnitude lower than the concentration of Na^+. Therefore, we implemented real-time compensation to calibrate the sensor readings based on their sensitivity to the non-target cations by using the calibration curves in Figure 5c (see the difference between "total response" and "response to cation", Figure 5d). Implementation of a compensation process thus ensured accurate readings. These results suggest that our OECT would be very capable of measuring excess concentrations of Na^+ and K^+ in complex media such as the blood.

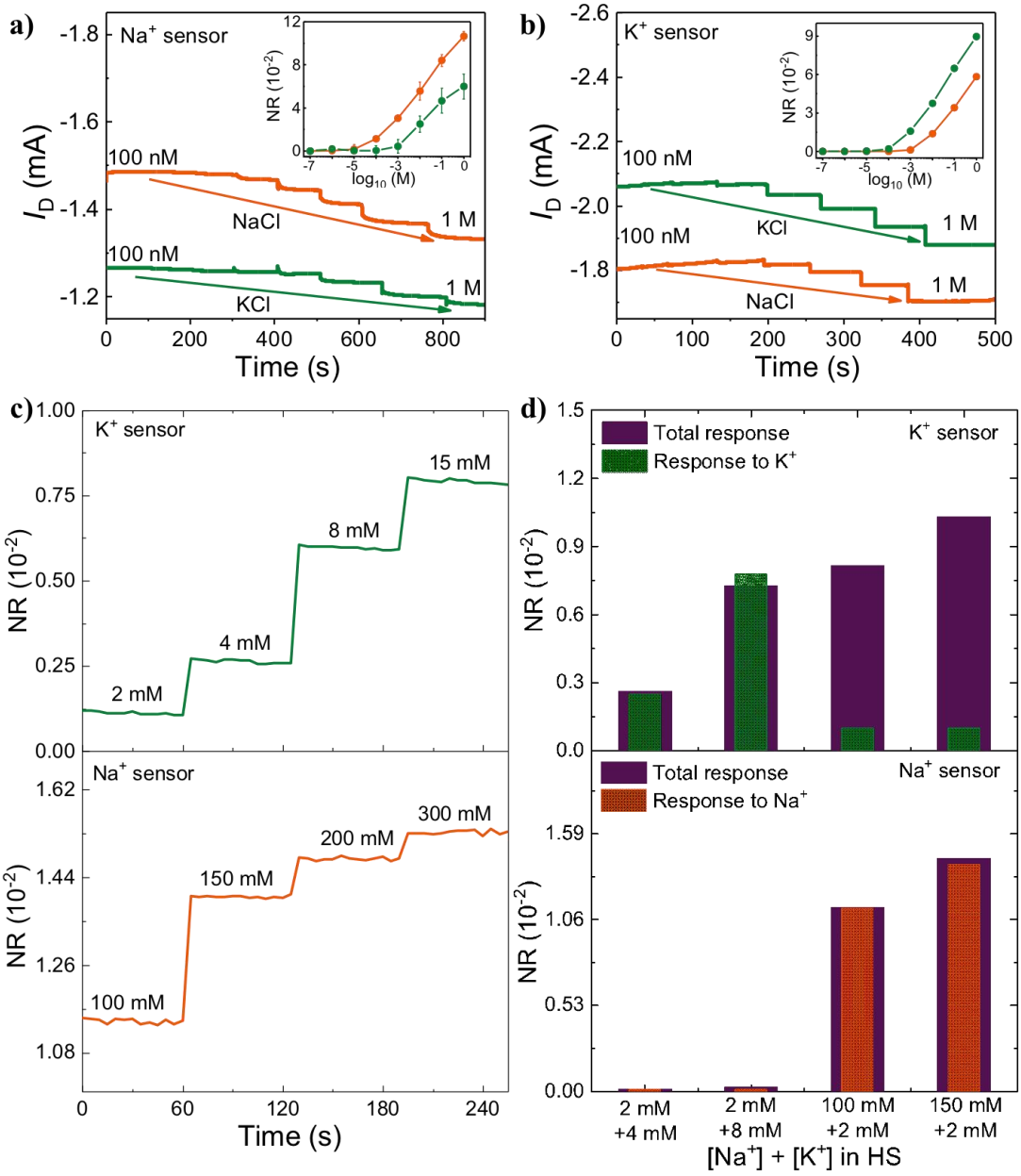

Figure 5. Real-time cation detection using the OECT. Real-time response of the **a)** Na^+ and **b)** K^+ sensors to a change in electrolyte concentration (NaCl, orange; and KCl, green) from 100 nM to 1 M. The error bars of the calibration curves shown in the inset were obtained from three devices. **c)** The NR of the multi-modal OECT to changes in Na^+ and K^+ concentrations in human serum (HS). **d)** System-level interference study: the NR of the OECT after a mixture of salts was added to HS (total response), and the compensated readouts showing the actual response of each sensor towards its target cation. V_D and V_G were -0.1 V for all the measurements.

In Table 1, we summarize the analytical characteristics of our ion-selective, multimodal OECT alongside the characteristics of two other state-of-the-art organic transistors developed for alkali-ion sensing. The ion-selective CP-gated OECT offered a lower voltage operation, as well as comparable linear range, sensitivity, and limit of detection (LOD) despite the absence of an ISM. Moreover, ISM-based ion sensors typically have a slow response time of several minutes, defined by the time the readout takes to reach equilibrium. The OECT reached a stable value within approximately 10 seconds, and the response time was independent of the ion concentration (Figure 5a-c).

Table 1. Comparison of organic thin-film transistor performances for alkali-metal ion sensing

Materials	Fabrication	ISM	Operation	Linear range (M)	Sensitivity (µA/dec)	LOD (M)	Ref.
P3HT	Spin coating	PVC*	V_D = -0.1 V V_G = -0.2 V	10^{-6} – 10^{-1}	0.25 – 0.5	10^{-6}	11
PEDOT:PSS	Drop casting	PVC*	V_D = -0.7 V V_G = 0 V	10^{-4} – 10^{-1}	47	1.5 x 10^{-5}	33
p(T15c5-*ran*-EDOT)	Electropolymerization	-	V_D = -0.1 V V_G = -0.1 V	10^{-5} – 1	37	2 x 10^{-5}	This work
p(T18c6-*ran*-EDOT)	Electropolymerization	-	V_D = -0.1 V V_G = -0.1 V	10^{-4} – 1	49	10^{-4}	This work

* PVC: polyvinylchloride

3. Conclusion

In summary, we developed conducting polymers that exhibited a rapid and selective electrical response to hydrated Na^+ and K^+ ions. The copolymer films were employed in two types of transducers and geometries: 1) amperometric, large-scale electrodes and 2) microfabricated OECTs. The porous morphology of the films attained with electropolymerization in the potentiostatic mode allowed the cations to readily and reversibly interact with the crown ethers,

as evidenced by Raman spectroscopy. The complexation of particular cations with the crown ether units of the copolymer led to a large reduction current. Designed as a single, miniaturized chip, the OECT enabled the selective detection of the two cations found in blood serum within a physiologically relevant range. The channel current changed in correlation with the number of cations intercalated by the ion-selective gate electrode. Notably, neither the electrodes nor the OECTs required a complex functionalization during fabrication, or ion-selective membranes to attain selectivity. Despite its simplicity and advantages, electropolymerization is however currently not fully compatible with up-scaling. On the other hand, assuming a progress which will ease the fabrication of microscale OECTs, the next decade will bring maturity to this technology. The tailor-made conducting polymers applied in OECTs thus have the potential to surpass existing technologies for the detection of alkali-metal ions in aqueous media. Future studies will focus on employing the OECTs in the form of implantable probes for niche applications such as in vivo monitoring of cations.

4. Experimental Section

Materials: We purchased 3,4-ethylenedioxythiophene (EDOT), tetrabutylammonium perchlorate (TBAP), dichloromethane (DCM), sodium chloride (NaCl), potassium chloride (KCl), lithium chloride (LiCl), ethylene glycol (EG), dodecyl benzene sulfonic acid (DBSA), (3-glycidyloxypropyl)-trimethoxysilane (GOPS), tetraethylene glycol ditosylate, acetonitrile (MeCN), sodium hydroxide (NaOH), tetramethylethylenediamine (TMEDA), and human serum from human male AB plasma from Sigma-Aldrich, and used all as received. The aqueous solutions were prepared using ultrapure water (Millipore Milli-Q). The ion-selective monomers were synthesized as detailed below and in the Supplementary Information.

Fabrication of the Ion-Selective CP Electrodes and OECTs: Our flexible substrates were based on a polyimide film (175 µm in thickness) that was cut into the circular geometry (d = 7

mm) shown in Figure 1. We sputtered a 10 nm of Cr layer as adhesion promoter and 100 nm thick Au layer on the top of the substrate, followed by sonication in acetone for 30 min, and electrochemical cleaning via cyclic voltammetry in 10 mM of H_2SO_4. The substrates were then soaked in ultrapure water and sonicated for 30 min before the electropolymerization of the CPs (detailed in section 2.3). The OECTs, on the other hand, were fabricated via photolithography using a Parylene-C (PaC) peel-off method, as previously reported.[33] The main steps of the device fabrication are illustrated in Figure S8. Briefly, we cleaned glass substrates by sonication in acetone/IPA solution, followed by O_2 plasma treatment. The photoresist S1813 was spin-coated onto the substrates, then exposed to UV light using a contact aligner, and developed using MF-319 developer. We deposited 10 nm Cr and 100 nm Au on the substrates using reactive metal sputtering. We performed lift-off by immersing the substrates in acetone/IPA mixture overnight. We deposited a 1.7 µm thick layer of PaC with an adhesion promoter to insulate the contacts. The second PaC layer was then evaporated, separated from the first one with a diluted soap coating (Micro-90) acting as an anti-adhesive. Photoresist AZ9260 and AZ developer were used in the following photolithography step. We opened the channels, gate patterns, and the contact pads using reactive ion etching. The six channels of one chip each had a width (W) of 100 µm and length (L) of 10 µm, while the two planar Au gate electrodes were 500 µm x 500 µm (Figure 1). The dispersion of poly(3,4-ethylenedioxythiophene) doped with a poly(styrene sulfonate) (PEDOT:PSS) (PH1000, Heraeus) containing EG (5 vol%), DBSA (0.25 vol%) and GOPS (1 wt%) was then cast on the channels. Upon soft baking at 140 °C for 1 min, the second PaC layer was peeled off. The coating on the gate area was gently removed with a cotton swab. The substrate was baked at 140 °C for 1 hour. Then, ion-selective CPs were electropolymerized on the gate contacts as described below.

Electropolymerization of the Ion-Selective CP Films: The ion-selective CP electrodes were prepared by electropolymerizing a mixture containing 100 mM of TBAP (the counter anion)

with different compositions of EDOT and T15c5 (Na^+-selective monomer) or T18c6 (K^+-selective monomer) in DCM. Either the flexible Au electrode or the planar Au gate electrode of the OECT was employed as the working electrode in a three-electrode configuration with a Pt counter electrode and an Ag/AgCl reference electrode, all immersed in the reaction mixture. We electropolymerized the films using a potentiostat (Autolab, PGstat128N, MetroOhm) under ambient conditions. To find the most sensitive electrode material possible, we tested three different electropolymerization modes: potentiodynamic (sweeping voltage), galvanostatic (constant current), and potentiostatic (constant voltage). Finally, we immersed the ion-selective CP-integrated devices in ultrapure water to remove any molecules that remained unbound to the surface and dried them using N_2 spray.

Characterization of the Ion-Selective CP Films: Fourier transform infrared (FTIR) spectra were recorded at room temperature in the range 500-4000 cm^{-1} using a Thermo Scientific Nicolet iS10. We used the attenuated total reflection (ATR) FTIR mode to obtain reflectance infrared spectra from the CP films coated on flexible electrodes as described above. We signal-averaged 64 scans to form a single spectrum displayed in terms of transmittance; the baseline was corrected using OMNIC FTIR software. Scanning electron microscope (SEM) images for a morphological analysis of the films were acquired using FEI Nova NanoSEM^{TM} microscope at an accelerating voltage of 3 kV and working distance of 5 mm. We recorded the Raman spectra using a LabRAM Aramin Raman spectrometer (Horiba Jobin Yvon) with an Olympus 50× objective on an automated *x–y* translation stage. A 633 nm helium–neon laser was used as the excitation source with a grating of 1800 g mm^{-1}. We performed 10 cycles at room temperature (21 °C) using an exposure time of 3 s to collect the data. All Raman spectra were baseline corrected. XPS experiments were performed using a KRATOS Analytical AMICUS instrument equipped with an achromatic Al Kα X-ray source (1468.6 eV). The source was operated at a voltage of 10 kV and current of 10 mA, generating thus 100 W power. The high-

resolution spectra were acquired using a step of 0.1 eV. The pressure in the analysis chamber during the whole measurement time was on the order of 10^{-7} Pa.

Charaterization of Ion Sensors: We performed cyclic voltammetry (CV) and chronoamperometry measurements using a potentiostat (Autolab PGstat128N, MetroOhm) with a standard electrochemical cell, in which the ion-selective CP was the working electrode, Ag/AgCl (in saturated KCl, 3 M) was the reference electrode, and a Pt wire as the counter electrode. The electrochemical measurements were carried out inside a grounded Faraday cage. We prepared electrolytes with varying concentrations of cations in water and added them subsequently to the cell, which held a constant electrolyte volume. For the chronoamperometry measurements, we applied a voltage pulse of -0.3 V *vs.* open circuit potential (V_{OC}) to the CP electrode for 60 s, and recorded the stabilized (non-capacitive) current in different electrolyte concentrations. We recorded the CV curves by sweeping the potential between -0.5 and 1.2 V *vs.* Ag/AgCl using a scan rate of 100 mVs^{-1}. We calculated the charge (Q) injected into the CP film using the area under the reduction current peak (I) in the CV curves, which was normalized by the scan rate (v) and deposited mass (m):

$$Q = \left| \frac{\int I.dV}{v.m} \right| \quad (2)$$

The steady-state OECT measurements (output and transfer curves) and the pulsed gate voltage experiments were performed using a Keithley 2612A controlled with customized LabVIEW software. We recorded the steady-state current by sweeping the gate voltage from -0.5 V to +0.6 V with the drain voltage changing from 0 to -0.6 V. For the pulsed gate-voltage experiments, the OECTs were operated at a constant drain voltage of -0.1 V and gate voltage of -0.1 V. In all the experiments, we monitored the gate and drain currents in real time upon exposure of the device to different concentrations of ions. For the human-serum experiments, we exposed the

OECT chip to samples with mixed concentrations of Na^+ and K^+, and measured the channel current using the Na^+-selective and K^+-selective gate electrodes integrated on the same chip (Figure 1). The response of the device (I_D at a set drain voltage, V_D = -0.1 V) to a variety of Na^+ concentrations operated at different gate voltages was normalized to allow for an accurate comparison among different conditions. The normalized response (NR) was determined by the following equation:

$$NR = \left|\frac{I - I_0}{I_0}\right| \quad (3)$$

where I and I_0 are the current outputs at a given electrolyte concentration and at the lowest electrolyte concentration tested (100 nM), respectively.[35]

Supporting Information

The Supporting Information is available free of charge on the Wiley website. (Synthesis of the monomers, electropolymerization curves, SEM images of the films prepared with different co-monomer rations, Raman and FTIR spectra of ion-selective films, OECT fabrication scheme steady state characteristics of ion-selective OECTs.)

Acknowledgements

This research was supported by King Abdullah University of Science and Technology (KAUST) Office of Sponsored Research Competitive Research Grants (CRG) OSR award number OSR-2016-CRG5-3003 to S. I. and I. M. Figure 1, inset of Figure 2a and TOC illustration were produced by Xavier Pita, scientific illustrator at KAUST.

Received: ((will be filled in by the editorial staff))
Revised: ((will be filled in by the editorial staff))
Published online: ((will be filled in by the editorial staff))

References

1. Chellan, P.; Sadler, P. J. The Elements of Life and Medicines. *Phil. Trans. R. Soc. A* **2015,** *373*, 2037.
2. Pohl, H. R.; Wheeler, J. S.; Murray, H. E. In *Interrelations between Essential Metal Ions and Human Diseases*; Sigel, A.; Sigel, H.; Sigel, R. K. O., Eds.; Springer Netherlands: Dordrecht, **2013**; pp 29-47.
3. He, F. J.; MacGregor, G. A. A Comprehensive Review on Salt and Health and Current Experience of Worldwide Salt Reduction Programs. *J. Hum. Hypertens.* **2008,** *23*, 363-384.
4. Gao, G.; Cao, Y.; Liu, W.; Li, D.; Zhou, W.; Liu, J. Fluorescent Sensors for Sodium Ions. *Anal. Methods* **2017,** *9* (38), 5570-5579.
5. Gooding, J. J.; Bakker, E.; Kelley, S. Should ACS Sensors Publish Papers on Fluorescent Sensors for Metal Ions at All? *ACS Sens.* **2016,** *1* (4), 324-325.
6. Wang, R.; Du, X.; Wu, Y.; Zhai, J.; Xie, X. Graphene Quantum Dots Integrated in Ionophore-based Fluorescent Nanosensors for Na^+ and K^+. *ACS Sens.* **2018**, DOI:10.1021/acssensors.8b00918 10.1021/acssensors.8b00918.
7. Ast, S.; Müller, H.; Flehr, R.; Klamroth, T.; Walz, B.; Holdt, H.-J. High Na^+ and K^+-induced Fluorescence Enhancement of a π-conjugated Phenylaza-18-crown-6-triazol-substituted coumarin Fluoroionophore. *Chem. Commun.* **2011,** *47* (16), 4685-4687.
8. Simeonov A, Davis MI. Interference with Fluorescence and Absorbance. 2015 Dec 7 [Updated 2018 Jul 1]. In: Sittampalam GS, Coussens NP, Brimacombe K, et al., editors. Assay Guidance Manual [Internet]. Bethesda (MD): Eli Lilly & Company and the National Center for Advancing Translational Sciences; 2004-.Available from: https://www.ncbi.nlm.nih.gov/books/NBK343429/
9. Bakker, E.; Pretsch, E. Peer Reviewed: The New Wave of Ion-Selective Electrodes. *Anal. Chem.* **2002,** *74* (15), 420-426.
10. Dimeski, G.; Badrick, T.; John, A. S. Ion Selective Electrodes (ISEs) and Interferences—A Review. *Clin. Chim. Acta* **2010,** *411* (5), 309-317.

11. Schmoltner, K.; Kofler, J.; Klug, A.; List-Kratochvil, E. J. W. Electrolyte-Gated Organic Field-Effect Transistor for Selective Reversible Ion Detection. *Adv. Mater.* **2013,** *25* (47), 6895-6899.
12. Gao, W.; Emaminejad, S.; Nyein, H. Y. Y.; Challa, S.; Chen, K.; Peck, A.; Fahad, H. M.; Ota, H.; Shiraki, H.; Kiriya, D. et al. Fully integrated wearable sensor arrays for multiplexed in situ perspiration analysis. *Nature* **2016,** *529*, 509-514.
13. Abramova, N.; Bratov, A. Photocurable Polymers for Ion Selective Field Effect Transistors. 20 Years of Applications. *Sensors* **2009,** *9* (9), 7097-7110.
14. Melzer, K.; Münzer, A. M.; Jaworska, E.; Maksymiuk, K.; Michalska, A.; Scarpa, G. Polymeric Ion-selective Membrane Functionalized Gate-electrodes: Ion-selective Response of Electrolyte-gated poly (3-hexylthiophene) Field-effect Transistors. *Org. Electron.* **2014,** *15* (2), 595-601.
15. Kim, Y.; Lim T..; Kim, C-H.; Yeo, C. S.; Seo, K.; Kim, S-M.; Kim, J.; Park, S-Y.; Ju, S.; Yoon, M-H. Organic electrochemical transistor-based channel dimension-independent single-strand wearable sweat sensors *NPG Asia Materials* **2018,** *10*, 1086-1095.
16. Lin, P.; Yan, F. Organic Thin-Film Transistors for Chemical and Biological Sensing. *Adv. Mater.* **2012**, *24 (1)*, 34-51.
17. Lin, P.; Yan, F.; Chan, H. L. W. Ion-Sensitive Properties of Organic Electrochemical Transistors. *ACS Appl. Mater. Interfaces* **2010,** *2* (6), 1637-1641.
18. Pedersen, C. J. Cyclic Polyethers and Their Complexes with Metal Salts. *J. Am. Chem. Soc.* **1967,** *89* (26), 7017-7036.
19. Bäuerle, P.; Scheib, S. Synthesis and Characterization of Thiophenes, Oligothiophenes and Polythiophenes with Crown Ether Units in Direct π-conjugation. *Acta Polym.* **1995,** *46* (2), 124-129.
20. Scheib, S.; Bäuerle, P. Synthesis and Characterization of Oligo- and Crown Ether-substituted Polythiophenes-A Comparative Study. *J. Mater. Chem.* **1999,** *9* (9), 2139-2150.

21. Marsella, M. J.; Newland, R. J.; Carroll, P. J.; Swager, T. M. Ionoresistivity as a Highly Sensitive Sensory Probe: Investigations of Polythiophenes Functionalized with Calix[4]arene-based Ion Receptors. *J. Am. Chem. Soc.* **1995,** *117* (39), 9842.

22. Marsella M. J.; Swager, T. M. Designing conducting polymer-based sensors: selective ionochromic response in crown ether-containing polythiophenes. *J. Am. Chem. Soc.* **1993,** *115* (23), 12214-12215.

23. Li, J.; Yim, D.; Jang, W.-D.; Yoon, J. Recent Progress in the Design and Applications of Fluorescence Probes Containing Crown Ethers. *Chem. Soc. Rev.* **2017,** *46* (9), 2437-2458.

24. Dabke, R. B.; Singh, G. D.; Dhanabalan, A.; Lal, R.; Contractor, A. Q. An Ion-Activated Molecular Electronic Device. *Anal. Chem.* **1997,** *69* (4), 724-727.

25. McQuade, D. T.; Pullen, A. E.; Swager, T. M. Conjugated Polymer-Based Chemical Sensors. *Chem. Rev.* **2000,** *100* (7), 2537-2574.

26. Si, P.; Chi, Q.; Li, Z.; Ulstrup, J.; Møller, P. J.; Mortensen, J. Functional Polythiophene Nanoparticles: Size-Controlled Electropolymerization and Ion Selective Response. *J. Am. Chem. Soc.* **2007,** *129* (13), 3888-3896.

27. Youssoufi, H. K.; Hmyene, M.; Garnier, F.; Delabouglise, D. Cation Recognition Properties of Polypyrrole 3-substituted by Azacrown Ethers. *J. Chem. Soc., Chem. Commun*. **1993**, 1550-1552.

28. Algı, F.; Cihaner, A. An Electroactive Polymeric Material and Its Voltammetric Response towards Alkali Metal Cations in Neat Water. *Tetrahedron Lett.* **2008,** *49* (21), 3530.

29. Giovannitti, A.; Nielsen, C. B.; Rivnay, J.; Kirkus, M.; Harkin, D. J.; White, A. J. P.; Sirringhaus, H.; Malliaras, G. G.; McCulloch, I. Sodium and Potassium Ion Selective Conjugated Polymers for Optical Ion Detection in Solution and Solid State. *Adv. Funct. Mater*. **2016,** *26* (4), 514-523.

30. Rivnay, J.; Inal, S.; Salleo, A.; Owens, R. M.; Berggren, M.; Malliaras, G. G. Organic Electrochemical Transistors. *Nat. Rev. Mater*. **2018,** *3*, 17086.

31. Ghittorelli, M.; Lingstedt, L.; Romele, P.; Crăciun, N. I.; Kovács-Vajna, Z. M.; Blom, P. W. M.; Torricelli, F. High-sensitivity Ion Detection at Low Voltages with Current-driven Organic Electrochemical Transistors. *Nat. Commun.* **2018,** *9* (1), 1441.
32. Cadogan, A.; Gao, Z.; Lewenstam, A.; Ivaska, A.; Diamond, D. All-solid-state Sodium-selective Electrode based on a Calixarene Ionophore in a Poly(vinyl chloride) Membrane with a Polypyrrole Solid Contact. *Anal. Chem.* **1992,** *64* (21), 2496-2501.
33. Sessolo, M.; Rivnay, J.; Bandiello, E.; Malliaras, G. G.; Bolink, H. J. Ion-Selective Organic Electrochemical Transistors. *Adv. Mater.* **2014,** *26* (28), 4803-4807.
34. Bernards, D. A.; Malliaras, G. G.; Toombes, G. E. S.; Gruner, S. M. Gating of an Organic Transistor through a Bilayer Lipid Membrane with Ion Channels. *Appl. Phys. Lett.* **2006,** *89* (5), 053505.
35. Bihar, E.; Wustoni, S.; Pappa, A. M.; Salama, K. N.; Baran, D.; Inal, S. A fully inkjet-printed disposable glucose sensor on paper. *npj Flex. Electron.* **2018,** *2* (1), 30.
36. Tyo, S.; Kazuaki, S.; Yoshihiro, O. Synthesis and Reductive Desulfurization of Crown Ethers Containing Thiophene Subunit. *Bull. Chem. Soc. Jpn.* **1989,** *62* (3), 838-844.
37. Cahiez, G.; Moyeux, A.; Gager, O.; Poizat, M. Copper-Catalyzed Decarboxylation of Aromatic Carboxylic Acids: En Route to Milder Reaction Conditions. *Adv. Synth. Catal.* **2013,** *355* (4), 790-796.
38. Hai, W.; Goda, T.; Takeuchi, H.; Yamaoka, S.; Horiguchi, Y.; Matsumoto, A.; Miyahara, Y. Specific Recognition of Human Influenza Virus with PEDOT Bearing Sialic Acid-Terminated Trisaccharides. *ACS Appl. Mater. Interfaces* **2017,** *9* (16), 14162-14170.
39. Bäuerle, P.; Scheib, S. Molecular Recognition of Alkali-ions by Crown-ether-functionalized Poly(alkylthiophenes). *Adv. Mater.* **1993,** *5* (11), 848-853.
40. Du, X.; Wang, Z. Effects of Polymerization Potential on the Properties of Electrosynthesized PEDOT Films. *Electrochim. Acta* **2003,** *48* (12), 1713-1717.

41. Xiao, R.; Cho, S. I.; Liu, R.; Lee, S. B. Controlled Electrochemical Synthesis of Conductive Polymer Nanotube Structures. *J. Am. Chem. Soc.* **2007,** *129* (14), 4483-4489.

42. Ouyang, L.; Wei, B.; Kuo, C.-c.; Pathak, S.; Farrell, B.; Martin, D. C. Enhanced PEDOT Adhesion on Solid Substrates with Electrografted P(EDOT-NH_2), *Sci. Adv.* **2017,** *3* (3), e1600448.

43. Morgan, W. E., Van Wazer, J. R., Stec, W. J., *J. Am. Chem. Soc.*, **1973**, *95*, 751-755.

44. Contat-Rodrigo, L.; Pérez-Fuster, C.; Lidón-Roger, J.; Bonfiglio, A.; García-Breijo, E. Characterization of Screen-Printed Organic Electrochemical Transistors to Detect Cations of Different Sizes. *Sensors* **2016,** *16* (10), 1599.

45. Wustoni, S.; Savva, A.; Sun, R.; Bihar, E.; Inal, S. Enzyme-Free Detection of Glucose with a Hybrid Conductive Gel Electrode. *Adv. Mater. Interfaces* **2018**, 1800928. https://doi.org/10.1002/admi.201800928.

46. Kim, S. H.; Hong, K.; Xie, W.; Lee, K. H.; Zhang, S.; Lodge, T. P.; Frisbie, C. D. Electrolyte-Gated Transistors for Organic and Printed Electronics. *Adv. Mater.* **2013,** *25* (13), 1822-1846.

47. Pin, P.; Saringkarinkul, A.; Punjasawadwong, Y.; Kacha, S.; Wilairat, D. Serum electrolyte imbalance and prognostic factors of postoperative death in adult traumatic brain injury patients *Medicine.* **2018,** *97* (45), e12081.

This work demonstrates, for the first time, a membrane-free electrochemical sensor for metal cations using all-polymer based electroactive material. The functionalized conducting polymer is fabricated via a single-step electropolymerization and employed either as an amperometric sensor or as a micrometer-scale gate electrode of an organic electrochemical transistor. At both configurations, the ion sensor offers selective and sensitive electrical sensing performance at low operation voltages.

Organic electrochemical transistors, bioelectronics, ion sensor, conjugated polymer, crown ether.

S. Wustoni, C. Combe, D. Ohayon, M.H. Akhtar, I. McCulloch, and S. Inal*

Membrane-Free Detection of Metal Cations with an Organic Electrochemical Transistor